MECHANICAL FORCE FIELDS IN A CLAY MINERAL PARTICLE SYSTEM

by

E. C. W. A. Geuze and Peter M. Rebull

The Winslow Laboratories
Rensselaer Polytechnic Institute
Troy, New York

ABSTRACT

Electrical double layer theory is used to analyze an idealized model unit of a clay particle system with the purpose of describing the mechanical stability in terms of an equilibrium of attractive and repulsive forces. Restricting the analysis to two dimensions, a symmetrical parallelogram formed by four typical clay mineral particles is taken as a representative unit of a flocculated clay and the interactions of mineral faces and associated electrolyte is investigated. The distortion energy of the system thus found is then directly related to the mechanical stability of the model unit's structure as it varies from parallel to perpendicular orientation. The general pattern of behaviour of the model unit will be shown to be compatible with the mechanical behavior of the clay mass.

INTRODUCTION

The mechanical interaction of the solid constituents of a clay mineral particle system obtained a theoretically justified basis through the work of Verwey and Overbeek (1948) on the interaction of two parallel plane double layers.

Since then contributions by several investigators have substantially increased our understanding of the mechanical behavior of systems composed of clay mineral particles and an electrolyte.

Obviously, a system composed of particles oriented in parallel, face-to-face positions only is rather the exception than the rule. Flocculated systems, in particular, have a geometrical structure of randomly oriented particles. The interaction of particles in these systems involves forces between the particle edges and the faces of their partners.

Van Olphen (1951) showed that at normal values of pH attraction forces resulted from the different charges on the faces (negative) and the edges (positive). Measuring the yield stress of clay gels, Van Olphen (1956) found the force of a single bond to be in the order of 10^{-4} dyne. Rausell-Colom (1958), on a theoretical basis, found the magnitude of electrostatic attraction between the (negative) face of montmorillonite and the unit charge on a contact edge to be in the order of 7×10^{-5} dyne.

https://doi.org/10.1346/CCMN.1966.0140110 Published online by Cambridge University Press

Norrish and Rausell-Colom (1963) investigated the swelling and compression of montmorillonite and vermiculite particle systems. They concluded that swelling of montmorillonite systems had to be limited by an opposing force system, which could not be explained by the Van der Waals attraction, as also previously stated by Rausell-Colom. The internal resistance to swelling of parallel, face-to-face systems was ascribed to the restraining effects of particles oriented in edge-to-face positions. From the results of compression and decompression tests of Na–montmorillonite systems it was concluded that a resistive force in the order of 6×10^4 to 6×10^5 dyne/cm^2 had to restrain the swelling. On this basis satisfactory agreement was found with the magnitude of a single edge-to-face bond as theoretically derived by Rausell-Colom. The same conclusion was reached by Van Olphen (1962) on the basis of earlier swelling experiments by Norrish (1954).

The concept of edge-to-face interaction, as a matter of course, is of foremost importance in an analysis of the structural forces in a flocculated system where particles occur in random orientations. In a general manner the force field can be separated into components of repulsion acting between opposite faces and components of attraction acting at the edges-to-faces.

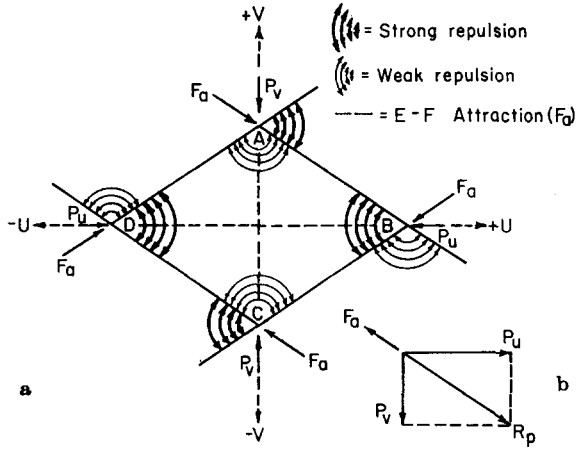


Figure 1a and 1b.

Each "cell" is supposed to be bounded by flat elements of mineral platelets; each corner of the cell is a meeting point of an edge and a face of a platelet. These cells are structural units which together form a framework of particles. The space occupied by the cells is filled with an electrolyte. We will assume that the faces of the platelets carry a uniform negative electric charge, whereas the edges carry an excess of positive electric charges. For the sake of simplicity the force field inside the cell and the forces acting on the

https://doi.org/10.1346/CCMN.1966.0140110 Published online by Cambridge University Press

platelets will be limited to a two-dimensional cell of "unit" thickness. In order to simplify the boundary conditions the cell has been given a symmetrical diamond shape.

THE POTENTIAL DISTRIBUTION IN THE CELL

The solution of this problem has been restricted to the application of double layers of the Gouy–Chapman type, i.e. assuming that Stern corrections are not required.

Following Verwey and Overbeek's treatment of the problem of interacting double layers of parallel plates, we have limited ourselves to a symmetrical electrolyte and assumed the validity of the Boltzmann theorem, whereby the charge density is given by:

$$\rho = ze(n_+ + n_-) = -2n \cdot z \cdot e \cdot \sinh(ze/kT)\psi \tag{1}$$

Assuming further the validity of Poisson's equation:

$$\nabla^2\psi = -\left(\frac{4\pi}{\epsilon}\right)\rho \tag{2}$$

and introducing the expression for ρ into the second equation, we obtain:

$$\nabla^2\psi = \left(\frac{4\pi}{\epsilon}\right)(2nze)\sinh(ze/kT)\psi$$

which in a two-dimensional problem yields:

$$\frac{\partial^2\psi}{\partial u^2} + \frac{\partial^2\psi}{\partial v^2} = \left(\frac{4\pi}{\epsilon}\right)(2nze)\cdot\sinh(ze/kT)\psi \tag{3}$$

Putting:

$$\left(\frac{4\pi}{\epsilon}\right)(2nze) = c_1 \tag{4}$$

$$ze/kT = c_2$$

Equation (3) is simplified to:

$$\frac{\partial^2\psi}{\partial u^2} + \frac{\partial^2\psi}{\partial v^2} = c_1 \cdot \sinh c_2\psi \tag{5}$$

where u and v are the Cartesian coordinates.

The solution of equation (5) with the appropriate boundary conditions is discussed in the Appendix.

THE INTERNAL EQUILIBRIUM OF A CELL

Equilibrium conditions of a two-dimensional cell of unit thickness obtained by an *E–F* association of particles, such as the one shown in Fig. 1a, depend on the combination of repulsive pressures and *E–F* attraction forces. We have adopted here the nomenclature proposed by Van Olphen (1963).

https://doi.org/10.1346/CCMN.1966.0140110 Published online by Cambridge University Press

The pressures acting on the planes of symmetry of the cell, as defined by the expressions in equations (12a) and (12b) of the Appendix, strongly depend on the angle α. The more acute the angle the higher the concentration of pressures on its bisecting plane. The pressures on the sides of the acute angle at A for instance, are many times larger than those on the sides of the complementary angle. The same consideration applies to the pairs of angles at B, C, and D. This distribution of pressures tends to rotate the sides of the cell until the angles are 90°, i.e. assuming that no other forces are active than those under consideration. Hence the concept of the cubic card-house structure as the limiting condition of internal equilibrium. To this concept should be added the requirement that the pressure on the plates balances the strength of the E–F bonds in order to represent a gel structure with a minimum of solid concentration. In general the E–F associations in a flocculated structure are randomly distributed throughout the system. [See, for instance, the distribution curves obtained with the low angle X-ray diffraction method by Norrish and Rausell-Colom (1963, p. 137).]

When a unit of the symmetrical diamond shape is subjected to a compressive force P_u in the u-direction and a force P_v in the v-direction the internal equilibrium requires that the pressures on the plane $v = 0$ balance the force P_v and that the pressures on the plane $u = 0$ balance the force P_u. When α is an acute angle P_u is considerably smaller than P_v. The ratio P_u/P_v is primarily a function of the angle α. This ratio has a lower limit and an upper limit depending on the strength of the E–F bonds. When the combined action of the pressures acting in the u-direction and the v-direction exceeds the attractive strength of the E–F bonds the unit loses its integrity and further deformations occur as a viscous flow (See Fig. 1b).

The behavior of clay systems subjected to decreasing p_u/p_v (pressure) ratios follows the analysis we presented above. In order to show the reversibility of the deformations, the imposed loads were completely released after each stepwise decrease of the ratio p_u/p_v. The curve in Fig. 2 shows the results of this procedure.

Variations of the hydrostatic pressure in the cell liquid were avoided by maintaining a constant value of the hydrostatic component of the imposed stresses. Since the clay was a cylindrical body:

$$p_0 = \tfrac{1}{3}(p_v + 2p_u)$$

with

p_0 = constant hydrostatic component of the state of stress.

The clay cylinder was therefore subjected to a stress deviator:

$$p_1 = p_v - p_0; \quad p_2 = p_u - p_0; \quad p_3 = p_u - p_0$$

with a maximum shear stress:

$$\tau = \tfrac{1}{2}(p_v - p_u)$$

Each step-wise increase of the deviator involved an increase of p_v of twice

https://doi.org/10.1346/CCMN.1966.0140110 Published online by Cambridge University Press

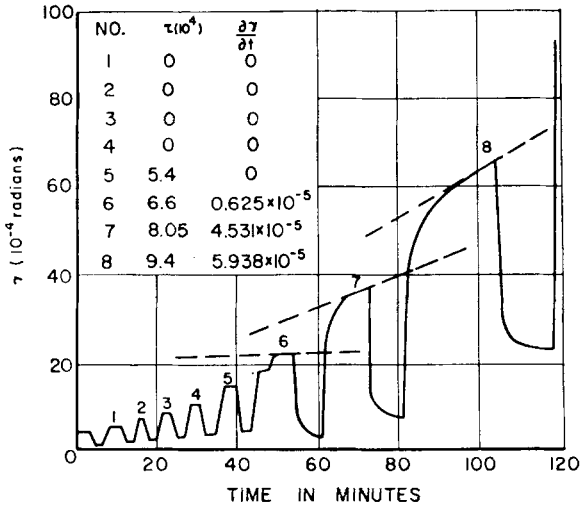


Figure 2.

the value of the decrease of p_u. Hence:

$$p_0 = \tfrac{1}{3}[(p_v + \Delta p_v) + 2(p_u - \Delta p_u)]$$

where:

$$\Delta p_v = -2\Delta p_u$$

and hence:

$$p_0 = \text{constant}$$

Each step increase of the shear stress was about 1.1×10^4 dyne/cm^2. The first five stress steps showed instantaneous, finite deformations with a small irreversible portion after unloading. It was known, however, that the material contained about $1\frac{1}{2}$ volume per cent of air. At the sixth step the transition from the stable structure to the flowing structure occurred. The next step and those following after that clearly showed the structural viscosity, which could be expressed in a rate of flow. The material behaved as a Bingham fluid:

$$\frac{\partial \gamma}{\partial t} = \frac{1}{\eta}(\tau - f_0) \tag{6}$$

where:

γ = shear or rotational strain

τ = shear stress

f_0 = yield stress

η = coefficient of structural viscosity

The results of the test are given in Fig. 3.

https://doi.org/10.1346/CCMN.1966.0140110 Published online by Cambridge University Press

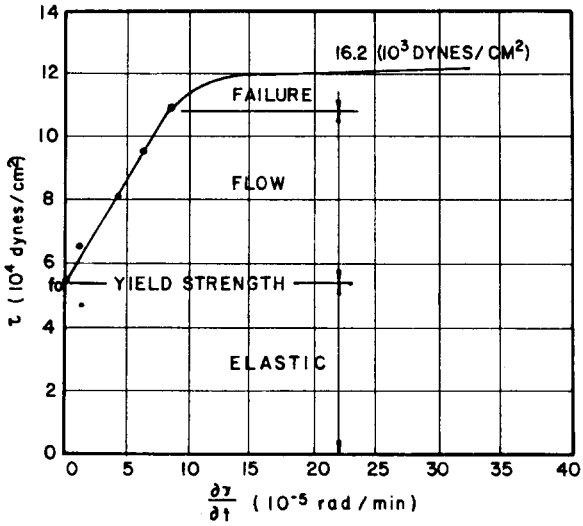


Figure 3

In consideration of the significance of the behavior of the material below the yield limit, two tests were performed on the same material. These results are shown in Fig. 4.

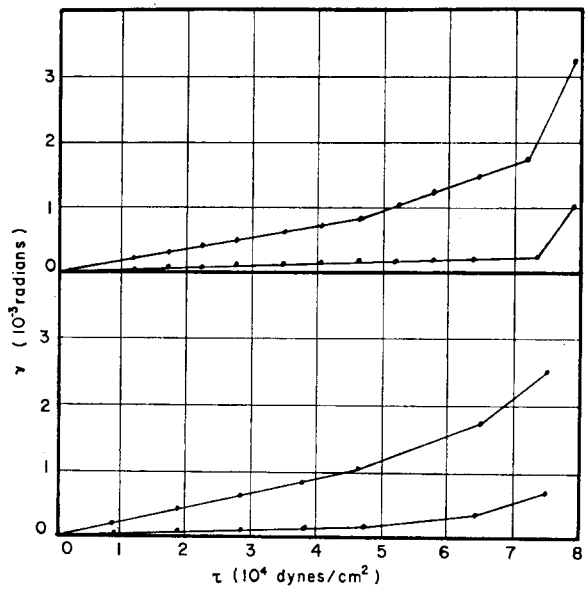


Figure 4

https://doi.org/10.1346/CCMN.1966.0140110 Published online by Cambridge University Press

In the first test the yield point showed clearly as a breaking point in the curve of the total strains and the irreversible strains at a stress of about 7×10^4 dyne/cm^2. This quantity compares rather well with the order of magnitude of the lower limit found by Norrish and Rausell-Colom in compression and decompression of Na–montmorillonite systems. In the second test the break is less pronounced and it occurs at a somewhat lower stress. The deformations also were slightly larger so that the structure probably lost part of its strength through the first run. The stress–strain relationships are clearly nonlinear and confirm as such the rotational character of the deformations.

LIQUID PRESSURES INDUCED BY STRUCTURAL DEFORMATIONS

The *E–F* associated structures are thus capable of withstanding deformation to a certain degree before the attractive bonds break. This fact has been demonstrated by investigators using different mechanisms, as has been mentioned in the introduction of this paper. It has, however, not been recognized that failure of attractive bonds may result from liquid pressures induced by structural deformations when the rate of strains imposed by the testing conditions does not permit the timely removal of the excess of interstitial liquid (Geuze, 1964).

Assuming a model cell as previously used, compression in the v-direction will be accompanied by an extension in the u-direction. The volume of the unit cell:

$$V = 2 \cdot L^2 \sin 2\alpha \tag{7}$$

and the change of its volume with respect to the angle α is:

$$\frac{dV}{d\alpha} = 4 \cdot L^2 \cos 2\alpha \tag{8}$$

Since in vertical compression $d\alpha$ is negative the change of volume is negative when $2\alpha < 90°$, whereas it is positive when $2\alpha > 90°$. In the first mentioned case the cell contracts; in the second case it dilates. The contraction of the cell cannot occur without stretching the bonds, if the liquid can be considered to be incompressible. Since both the electrostatic and the Van der Waals attraction forces are inversely proportional to a high power of the distance between the edges and the faces, a comparatively small compressive strain will cause breaking of the bonds.

In the test discussed in the previous chapter drainage of the liquid from the system was prevented at the boundaries. Hence the change of volume was a negligible quantity. The rotation at the yield point was about 2×10^{-3} radians, but since the average angle 2α was unknown we have no means of checking this result.

When drainage of the system is permitted, the attractive bonds will not only develop to their fullest extent, but the edges may even approach the

https://doi.org/10.1346/CCMN.1966.0140110 Published online by Cambridge University Press

faces at closer distances because the particles are pressed together. The removal of part of the electrolyte affects the charge distribution inside the cell. The establishment of a new electrical equilibrium takes a certain time, depending on the mobility of the ions. In the new equilibrium the contact forces depend on the repulsive forces, which will then be increased. Obviously, the approach to a new equilibrium requires very low rates of deformation in order to keep in step with the movements of the ions.

When, on the other hand, drainage is allowed for but the rate of deformation is high, the bonds in a contracting system will be stretched by the increase of the liquid pressure. The yield strength will then depend on the hydrostatic pressure in the cells. Because the latter is an all-sided equal internal pressure it is to be superimposed on the repulsive pressure system. As a result the clay system will show a lower yield strength. This conclusion seems to contradict the general experience of increasing strength of clays at high rates of loading. It should be emphasized in this context that "strength" is then referred to as failure of the system. As shown in Fig. 3 failure is preceded by a wide range of flow. This range is defined by equation (6) from which it follows that the difference between the shear stress and the yield stress is proportional to the rate of flow. In other words, the resistance of the material increases at the expense of a high rate of flow. Equation (6), however, does not account for the fact that the strength depends on the magnitude of the strain preceding failure. It seems that the smaller the strain that can be obtained by a quick succession of load increases, the higher the failure strength. In a sense the material is forced to behave as brittle materials, which show small strains at the point of failure.

Summarizing the major part of the above statements, we arrive at the conclusion that the yield strength of a clay system decreases when the rate of deformation is increased, but that the failure strength increases as a result of the participation of the structural viscosity. In any type of measurement of the yield strength these complications should be avoided. It seems that the solution of the problem lies in the application of loading programs involving small increments of stress followed by a complete release of stress in order to study the reversibility of the strains. The loading and unloading sequences should be carried out at a slow rate to enable the strains to reach their final, at rest values.

DISCUSSION

The use of a symmetrical unit of particles in *E–F* association has obvious advantages in studying the internal equilibrium of the cell. External compressive forces are balanced with the repulsive forces and through this balance it is possible to evaluate the deformation of a symmetrical unit.

The assumption of rigid platelets, however, is a severe limitation of the analysis, which is approximately correct when the platelets are stretched by an internal hydrostatic pressure. Compressive forces may cause bending,

https://doi.org/10.1346/CCMN.1966.0140110 Published online by Cambridge University Press

buckling and folding of the platelets. These deformations introduce a force system which cannot be readily accounted for. In a flocculated system cells of various sizes and shapes constitute a continuous network. Each of these cells occurs in a state of internal equilibrium. When the entire system is subjected to an external force, the internal mechanical forces acting at the particle contacts depend on the relative rigidity of the units as a whole and not on the internal repulsive pressures only. The contact forces, furthermore, participate in the distribution of the force system in an unknown manner.

It is therefore a remarkable fact that the model cell shows a mechanical behavior which is identical with that of most clay systems.

The combination of the repulsive forces, based upon the interaction of diffuse double layers, and the edge-to-face attraction forces proved to be essential in explaining the elastic, nonlinear behavior of the flocculated system within the yield range. This behavior is in many ways identical with that of a model of parallel plates with cross-links, as proposed by other investigators.

The measurement of the attraction bonds is not a simple procedure. Yet, lacking sufficiently accurate methods for the evaluation of the electric charge on the particle edges, the direct experimental method is a necessity.

CONCLUSIONS

The solution of the two-dimensional problem of the potential distribution in a Poisson–Boltzmann electrical field is possible when using a numerical difference approximation method. The boundaries of the field are assumed to be platelets carrying a uniform negative charge. The liquid pressure distribution on the platelets is obtained from the potential distribution along the planes of symmetry. The internal equilibrium of forces inside a "cell" surrounded by platelets depends on the balance between the liquid pressures induced by the interaction of the diffuse double layers and the attraction forces between the edges and the faces of the platelets. When the cell is subjected to compressive forces acting in the direction of the planes of symmetry the deformation of the cell increases the repulsive forces in the direction of the compression and decreases the repulsive forces in the direction of the extension. In this manner the cell is capable of withstanding external forces at the expense of deformation (rotations). At the same time the edges of the plates approach their opposite faces. Deformations performed at a high rate (as, for instance, in rotation viscometers) cause liquid pressures in the system, when the cells tend to contract by the deformation. These pressures have to be superimposed on the liquid pressures induced by the electrical forces and may cause rupture of bonds. As a result high rate deformation tests tend to lower the strength of the bonds and to increase the resistance by structural viscosity. The best approximation of the yield strength is by the application of small stress increments, each one followed by a complete release of stress in order to show the integrity of the particle

https://doi.org/10.1346/CCMN.1966.0140110 Published online by Cambridge University Press

structure by the reversibility of the strains. The rate of application of the subsequent stress steps and releases should be slow enough to enable the strains to reach their final, at rest values.

REFERENCES

GEUZE, E. C. W. A. (1964) The uniqueness of the Mohr–Coulomb concept in shear failure: in *Laboratory Shear Testing of Soils*, ASTM Special Tech. Pub. No. 361, 52–64.

NORRISH, K. (1954) The swelling of montmorillonite: *Disc. Faraday Soc.*, No. 18, 120–34.

NORRISH, K., and RAUSELL-COLOM, J. A. (1963) Low-angle X-ray diffraction studies of the swelling of montmorillonite and vermiculite: *Clays and Clay Minerals*, Proc. 10th Conf., Pergamon Press, New York, 123–49.

RAUSSELL-COLOM, J. A. (1958) El hinchamiento de la montmorillonita-sodica y del complejo montmorillonita-krilium en electrolitos: Doctoral thesis, Univ. of Madrid.

VAN OLPHEN, H. (1951) Chemical treatment of drilling fluids: Thesis, Delft, 137 pp.

VAN OLPHEN, H. (1956) Forces between suspended bentonite particles: *Clays and Clay Minerals*, Proc. 4th Conf. Natl. Acad. Sci.—Nat. Res. Council Pub. 456, 204–24.

VAN OLPHEN, H. (1962) Unit layer interaction in montmorillonite systems: *Jour. Coll. Sci.*, 17, 660–667.

VAN OLPHEN, H. (1963) *An Introduction to Clay Colloid Chemistry:* Interscience, New York, 301 pp.

VERWEY, E. J. W., and OVERBEEK, J. TH. G. (1948) Elsevier Publishing Company, Amsterdam, 205 pp.

APPENDIX

THE POTENTIAL FIELD

The potential distribution satisfies:

$$\frac{\partial^2 \psi}{\partial u^2} + \frac{\partial^2 \psi}{\partial v^2} = c_1 \sinh(c_2 \psi) \tag{1}$$

The region is defined as the quarter space of the diamond.

The length L of the hypotenuse and the angle α are the geometrical parameters of the rectangular triangle OAB. The coordinate planes $v = 0$ and $u = 0$ are the rectangular sides OB and OA respectively (Fig. 5).

The boundary conditions are for reasons of symmetry:

$$\text{on the plane } u = 0: \qquad \frac{\partial \psi_{u_0}}{\partial u} = 0 \tag{2a}$$

$$\text{on the plane } v = 0: \qquad \frac{\partial \psi_{v_0}}{\partial v} = 0 \tag{2b}$$

where ψ_{u_0} and ψ_{v_0} are the potentials on the coordinate planes $u = 0$ and $v = 0$ respectively.

The boundary condition along the hypotenuse is defined by the postulate of a uniform (negative) charge on the plate. The charge on the plate is pro-

https://doi.org/10.1346/CCMN.1966.0140110 Published online by Cambridge University Press

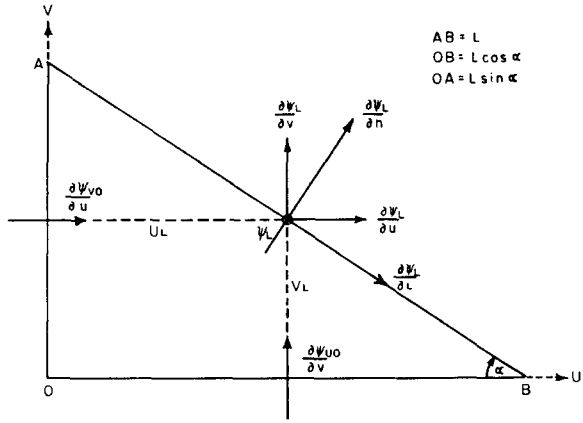


Figure 5.

portional to the negative value of the potential gradient at points on the boundary in the direction of the positive normal to the hypotenuse:

$$\frac{\partial \psi_L}{\partial n} = -\frac{\epsilon}{4\pi} \cdot \sigma_0 \tag{3}$$

where ψ_L is the potential at points along the boundary and σ_0 is the (negative) charge on the plate.

The potential gradient is related to its components in the u-direction and the v-direction by:

$$\frac{\partial \psi_L}{\partial n} = \sin\alpha \cdot \frac{\partial \psi_L}{\partial u} + \cos\alpha \cdot \frac{\partial \psi_L}{\partial v} \tag{4a}$$

The solution of the partial differential equation (1) with the boundary conditions (2a), (2b) and (3) required the use of a numerical integration method. A modification of the Newton–Raphson method, as proposed by the junior author, yielded results of sufficient accuracy.

THE PRESSURE ON THE PLATE

The objective of computing the potentials was to provide the quantities required for obtaining the liquid pressure distribution on the boundary plate.

The liquid pressure gradient balances the electrical force on the space charge at every point in the region under equilibrium conditions:

$$\text{grad}\, p = -\rho \cdot \text{grad}\, \psi \tag{5}$$

In a two-dimensional space we have two gradient components at every point:

$$\frac{\partial p_u}{\partial u} = -\rho \cdot \frac{\partial \psi}{\partial u} \tag{6a}$$

https://doi.org/10.1346/CCMN.1966.0140110 Published online by Cambridge University Press

and

$$\frac{\partial p_v}{\partial v} = -\rho \cdot \frac{\partial \psi}{\partial v} \tag{6b}$$

where p_u and p_v are the liquid pressures acting in the u-direction and in the v-direction respectively. The pressure increments over elementary distances du and dv are:

$$dp_u = -\rho \cdot d_u\psi \tag{7a}$$

and

$$dp_v = -\rho \cdot d_v\psi \tag{7b}$$

Introducing the expression for ρ from equation (1) using the coefficients from equations (4), yields:

$$\rho = -\left(\frac{\epsilon}{4\pi}\right)c_1 \sinh(c_2\psi)$$

Hence:

$$dp_u = \frac{\epsilon}{4\pi}\left(\frac{c_1}{c_2}\right)d_u \cosh(c_2\psi) \tag{8a}$$

$$dp_v = \frac{\epsilon}{4\pi}\left(\frac{c_1}{c_2}\right)d_v \cosh(c_2\psi) \tag{8b}$$

Integration of these expressions between the limits indicated in Fig. 6:

$$u = 0; \quad p_u = p_{u0}; \quad \psi_u = \psi_{u0}$$
$$u = u_L; \quad p_u = p_{u0}; \quad \psi_u = \psi_L$$

and

$$v = 0; \quad p_v = p_{v0}; \quad \psi_v = \psi_{v0}$$
$$v = v_L; \quad p_v = p_{vL}; \quad \psi_v = \psi_L$$

yields:

$$\int_{P_{uo}}^{P_{uL}} dp_u = \left(\frac{\epsilon}{4\pi}\right)\frac{c_1}{c_2}\int_{\psi_{uo}}^{\psi_L} d_u \cosh(c_2\psi)$$

and

$$\int_{P_{vo}}^{P_{vL}} dp_v = \left(\frac{\epsilon}{4\pi}\right)\frac{c_1}{c_2}\int_{\psi_{vo}}^{\psi_L} d_v \cdot \cosh(c_2\psi)$$

The pressure differences are:

$$p_{uL} - p_{u0} = \left(\frac{\epsilon}{4\pi}\right)\frac{c_1}{c_2}\left[\cosh(c_2\psi_L) - \cosh(c_2\psi_{u0})\right] \tag{9a}$$

$$p_{vL} - p_{v0} = \left(\frac{\epsilon}{4\pi}\right)\frac{c_1}{c_2}\left[\cosh(c_2\psi_L) - \cosh(c_2\psi_{v0})\right] \tag{9b}$$

https://doi.org/10.1346/CCMN.1966.0140110 Published online by Cambridge University Press

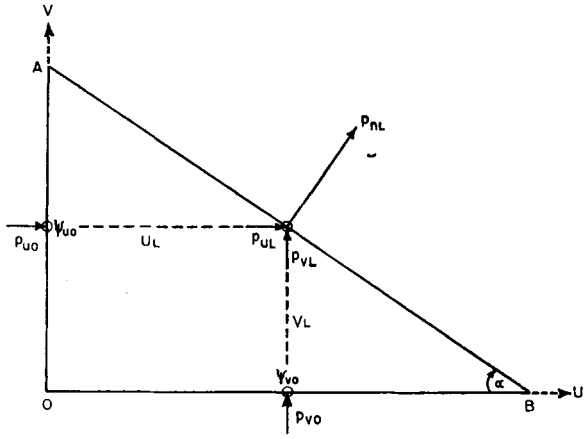


Figure 6.

These differences are balanced by the electrical forces acting on the space charges between the respective boundaries in the u-direction and in the v-direction. They do not contribute to the pressures acting on the plate. From the equilibrium conditions of the triangular space OAB it follows, however, that the pressures p_{u0} and p_{uv} are transmitted by the liquid to the plate. The equilibrium conditions of an elementary triangle of the liquid

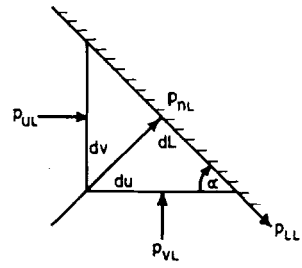


Figure 7.

with sides du, dv, and dL are schematically represented in Fig. 7. These can be expressed as follows:

$$p_{nL} = p_{uL} \cdot \sin^2\alpha + p_{vL} \cdot \cos^2\alpha \tag{10}$$

Since $p_{uL} = p_{u0}$ and $p_{vL} = p_{v0}$, equation (10) can be written:

$$p_{nL} = p_{u0} \cdot \sin^2\alpha + p_{v0} \cdot \cos^2\alpha \tag{11}$$

where:

$$p_{u0} = \frac{\epsilon}{4\pi}\left(\frac{c_1}{c_2}\right)\cosh(c_2\psi_{u0}) \tag{12a}$$

https://doi.org/10.1346/CCMN.1966.0140110 Published online by Cambridge University Press

$$p_{v_0} = \frac{\epsilon}{4\pi}\left(\frac{c_1}{c_2}\right)\cosh(c_2\psi_{v_0}) \tag{12b}$$

Hence:

$$p_{nL} = \frac{\epsilon}{4\pi}\left(\frac{c_1}{c_2}\right)[\sin^2\alpha\cdot\cosh(c_2\psi_{u_0}) + \cos^2\alpha\cdot\cosh(c^2\psi_{v_0})] \tag{13}$$

The liquid pressures from equations (12a) and (12b) should not be confused with the osmotic pressures, which are required to maintain the balance between the potentials in the planes of symmetry of the diamond, i.e. the planes $u = 0$ and $v = 0$, and the zero potential of an electrolyte reservoir.

Because the diamond is a self-contained unit in electrical and mechanical equilibrium, such a reservoir is not required to maintain the internal balance of forces.

https://doi.org/10.1346/CCMN.1966.0140110 Published online by Cambridge University Press